

2-2008

Thermal Damage Approach of Concrete: Application to Specimens Subjected to Combined Compressive and High Temperature Loads

Abdellah Menou
University of Dayton


Ghassan Mounajed
MOCAD Division

Hocine Boussa
MOCAD Division

Christian La Borderie
Univ. Pau et Pays de l'Adour

Khalid Lafdi
University of Dayton, klafdi1@udayton.edu

Follow this and additional works at: https://ecommons.udayton.edu/cme_fac_pub

 Part of the [Other Chemical Engineering Commons](#), [Other Materials Science and Engineering Commons](#), [Polymer Science Commons](#), and the [Structural Materials Commons](#)

eCommons Citation

Menou, Abdellah; Mounajed, Ghassan; Boussa, Hocine; La Borderie, Christian; and Lafdi, Khalid, "Thermal Damage Approach of Concrete: Application to Specimens Subjected to Combined Compressive and High Temperature Loads" (2008). *Chemical and Materials Engineering Faculty Publications*. 33.
https://ecommons.udayton.edu/cme_fac_pub/33

This Article is brought to you for free and open access by the Department of Chemical and Materials Engineering at eCommons. It has been accepted for inclusion in Chemical and Materials Engineering Faculty Publications by an authorized administrator of eCommons. For more information, please contact frice1@udayton.edu, mschlangen1@udayton.edu.

Thermal Damage Approach of concrete: Application to Specimens Subjected to Combined Compressive and High Temperature Loads

A. Menou^{1,4,*}, G. Mounajed², H. Boussa², Ch. La Borderie³, Kh.Lafdi¹

¹UDRI Carbon, University of Dayton, USA,

²MOCAD Division – CSTB, France,

³LaSAGeC, Univ. Pau et Pays de l'Adour, France, ⁴AIMAC/ONDA, Casablanca-Morocco

(Received November 12, 2007 ; final form November 23, 2007)

ABSTRACT

Within the framework of study of concrete structures subjected to fire, a theoretical and experimental work was conducted. The aim of this study was to investigate and to model the damage mechanisms of concrete after their exposure to high temperatures. The multiphase Digital Concrete Model as well as the damage model, MODEV, which were both implemented on the finite-element software package, SYMPHONIE, were used simultaneously to assess the thermal damage of the concrete. In order to validate the thermal damage model, an experimental investigation was performed. The mechanical characteristics of 5 cementitious materials, which included cement paste, mortar, ordinary concrete and 2 HSC concretes, were measured with 3-point bending tests immediately succeeding heating/cooling cycles of 393, 523 and 673 K.

The experimental tests on the 3 different materials were then compared to the numerical simulations and are presented for temperatures up to 673 K.

Several applications were investigated after the validation of the models, one of which was the fire resistance of concretes when simultaneously subjected to both compressive and high temperature loads.

Keywords: thermal damage, high temperature, concrete model, cement paste, micro-macro.

1. INTRODUCTION

The present work was conducted within the framework of the study of concrete behaviour at high temperatures. The experimental studies illustrate the important influence that temperature has on the behaviour of concretes, particularly High-Strength Concretes (HSC). The need to design durable concrete structures, fuels the need for sophisticated modeling of their respective deterioration phenomena. Thus, it is essential to consider the coupling and the nonlinearity of the processes involved in the degradation mechanisms of these concrete materials.

Several experimental research studies including the famous works of Bazant and Prat /1/, Diederich *et al.* /2/ and Ulm *et al.* /3/ have highlighted the complexities of the behaviour of concrete when subjected to high temperature. This work shows the existence of a combination of damage mechanisms stemming from the following origins: mechanical (strain), physical (heat transfer, free water transfer, variation of conductivity, etc.) and chemical (dehydration, carbonization, chemical transformations, etc.).

Concrete is a highly heterogeneous material that can be quantified in three levels: macroscale, mesoscale and microscale as using by Brandt /4/ and Van Mier /5/. The heterogeneity is one of the main reasons that cause the concentration stress and local failure. Although at room

* Corresponding author. Tel.: +33 238255056; Fax: +33 238257825; E-mail addresses: abdellah.menou@univ-pau.fr

temperature, the effects of heterogeneity on the fracture processes in concrete have been reported in literatures by Brandt /4/ and Tijssens *et al* /6/, these studies did not consider the effects of heterogeneity among the phase materials of concrete on the stress development and cracking process under high temperatures.

The objective of this particular theoretical and experimental study is to identify the elementary mechanisms leading to the deterioration of concrete under the effect of temperature, and to propose a model that will predict and evaluate the damage assessed by high temperatures on the different forms of concrete. In the theoretical model, we consider that the observed global damage can be broken up into thermal damage of a mechanical origin caused by non-free thermal strain (at the macroscopic and microscopic levels), and additional thermal damage (not accompanied by strain) caused by the physical and chemical transformations of the material.

In this research, the microscopic multi-phase Digital-Concrete F.E. model (DC), and the macroscopic deviatoric damage model, MODEV, were used to evaluate the thermal damage at both the macroscopic and microscopic levels. These two models were then implemented in the general finite element code SYMPHONIE by Mounajed /7/. The multi-scale approach presented here allows for a better understanding of the elementary mechanisms behind the thermal deterioration of the concrete, while highlighting the effect of the differential thermal expansion between the cement paste and related aggregates. Using the two previous models as a foundation, a new approach to the thermal damage of concretes is presented.

2. MULTI-SCALE APPROACH

2.1. Principles of the Multi-Scale Identification of Concrete Thermal Damage

The thermal damage of concrete represents a specific mechanism directly associated to the nature of this heterogeneous material. Analysis of the different standard macroscopic models illustrates how insufficient these models are with respect to the representation of the complex mechanisms involving concrete thermal damage. All concrete macroscopic

models assume homogeneity, thus having a free displacement specimen that is subjected to a uniform thermal load, which expands without stresses and elastic strains and does not exhibit mechanical damage. Conversely, experiments conducted in laboratories, show that the thermal damage process of concrete actually begins at relatively low temperatures, even when involving a homogeneous material.

This study proposes a new approach to studying the thermal damage of concrete. This approach was based on the multi-scale homogenization of concrete using the Digital Concrete model. Several scales of modelling were taken into account, including cement paste and other concrete materials, and these scales were formulated explicitly from the works of Mounajed *et al.* /8,9/. Thus, the concrete is considered to be a combination of three materials: concrete, mortar, and cement. Each material is judged on its specific scale and made into a homogenous mixture prior to proceeding to the next scale and being homogenized again. Figure 1 shows the basis of this approach. The mechanical and thermal characteristics of cement paste and sand aggregates are conjointly introduced into the Digital Concrete DC model in order to homogenize the mortar's behaviour. This process is repeated for concrete homogenization by introducing the characteristics of the homogenized mortar and the aggregates, obtained in the previous step into the DC model. This step provides insight into the thermo-mechanical behaviour of concrete. The local DC model uses a random approach to generate the internal structure of a heterogeneous material, such as concrete, mortar or cement paste, on a smaller scale. The proposed approach considers a multi-phase material, with successions of n phases, spatially distributed in a random manner. To represent concrete, the following two phases are taken into account: 1st phase: Solid skeleton of the matrix cement P1; 2nd phase: A random distribution of aggregates with the possibility of analyzing this phase in n sub-phases in order to represent different sizes and natures of aggregates P21, P22... P2n.

2.2. Thermal Damage Model

The basic mechanisms leading to the thermal damage of concrete have been divided into two main

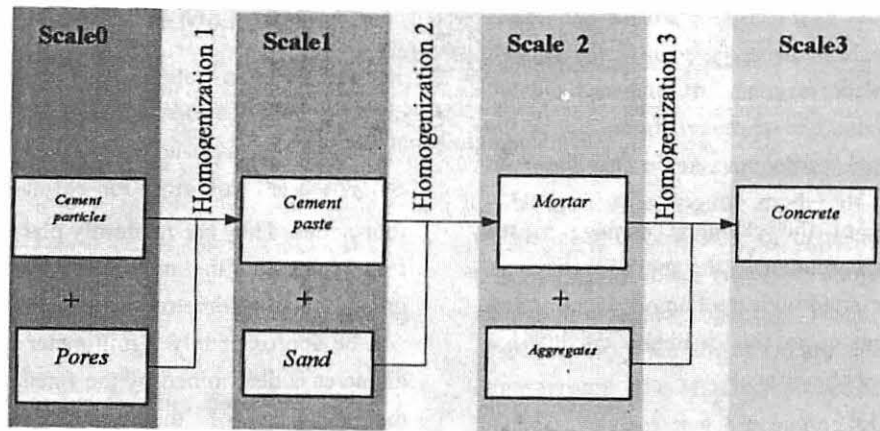


Fig. 1: Different phases for homogenization

categories in the present approach and are discussed in the succeeding sections.

a. Mechanical damage stemming from a thermal origin, accompanied with strains and due to the restrained thermal strains on a macroscopic and microscopic scale include the following: The original mechanical damage could be the temperature gradient, the boundary conditions, the geometric shape on a macroscopic scale, or even the differential expansion between the cement paste and the aggregates at a microscopic scale. This damage is decomposed into mechanical, macroscopic damage, d_{macro} , and mechanical microscopic damage, d_{micro} .

The mechanical-thermal damage of concrete was modelled with the deviatoric damage model, MODEV, which is based both on the damage mechanics and thermodynamics approach. The model uses a non-symmetrical criterion in strain and introduces 2 scalar equivalent strains representing local sliding and crack opening, respectively. They are calculated from the deviatoric and spherical parts of the strain tensor. The MODEV model also considers 2 scalar damage variables, corresponding respectively to the sliding and crack opening degradation mechanisms. Each damage variable has its own evolution law. The damage variables are independent from the temperature and can be obtained directly from the mechanical behaviour law.

b- Purely thermal damage without strains due to the different chemical transformations that occur mainly in cement paste include dehydration, important mass

loss beyond 120°C, and other chemical transformations. The physical and chemical changes in concrete under high temperatures depend not only on the matrix composition, but also on the type of aggregate (mineralogical characteristics, dilatation, etc.). Other influential factors include the water/cement ratio, the porosity, the humidity and the age of concrete. As the cement paste is exposed to increasing temperatures, the following effects can be distinguished: expulsion of evaporable water (373 K), the beginning of the dehydration of the hydrate calcium silicate (453 K), the decomposition of calcium hydroxide (793 K) and the decomposition of the hydrate calcium silicate (that begins around 973 K). The alterations produced by high temperatures are more evident when the temperatures surpass 793 K. This damage has been identified from the tests performed on the cement samples in this study. In this method, we consider several scales of modelling, ranging from the cement paste to the concrete material. Thus, the concrete is considered as a combination of three materials: cement, sand, and aggregates. Each material is considered on its specific scale, and homogenization is needed on each scale to proceed to the remaining succeeding scales. **Figure 2** shows the basis of this approach.

The chemical damage in the cement paste, g , is the only part of the total damage that should be identified through experiments in this approach. The mechanical and thermal characteristics of sand aggregates were jointly injected into the Digital Concrete DC model



Fig. 2: Digital concrete model

with the evolution of the chemical damage in the cement in order to homogenize the mortar behaviour. This process is continued with the homogenized mortar and concrete aggregates to finally obtain the thermo-mechanical concrete behaviour.

3. THE BASIS OF THE UTILIZED MODEL

In this section, the basis for the Digital Concrete (DC) model and the MODEV damage model that were implemented into SYMPHONIE F.E. code and used simultaneously to identify the thermal damage of concrete is discussed.

3.1 The DC Microscopic Model

The local DC model considers a random approach to generate the internal structure of the heterogeneous materials like concrete, mortar or even cement paste on a smaller scale. The proposed approach allows the consideration of the Digital Concrete as a multi-phase material with successions of n phases spatially distributed in a random manner.

$$DigitalConcrete = \sum_i^{nb \text{ phases}} \text{phase} \times Volume_i$$

For the present simulations, the following phases were adopted to represent concrete:

1st phase: Solid skeleton of the matrix cement, P_1

2nd phase: A random distribution of pores with the possibility of analyzing this phase in n sub-phases to represent different volumes and natures of pores $P_{21}, P_{22}, \dots, P_{2n}$

3rd phase: A spatial random distribution of aggregates with the possibility of analyzing this phase in m sub-phases to take into account the different sizes and different natures of aggregates P_{31}, \dots, P_{3m}

The 2-dimensional mesh is composed of plane stress elements. The elements are quadrilaterals, each with

four nodes. They are randomly placed to prevent cracks from following the mesh pattern. Since the smallest grains are 4 millimetres in diameter, the element sides will be approximately 1 millimeter each. The minimum diameter is determined by the fineness of the mesh, and the diameter of the smallest grain has to be approximately twice the that of the element size. This relation is reversible: when smaller grains need to be simulated, the element size can be adjusted accordingly. The maximum diameter should not be larger than approximately one third of the total specimen size to prevent the random placement of the particles from changing the behaviour of the specimen. When the maximum diameter is larger, the specimen must also be larger. Of course, both for minimum and maximum diameters of the grains, it is important to notice that an increase in the number of elements will largely increase the calculation time. For this reason, the range of particle diameters will be limited to approximately a factor 4 between the smallest and the largest grains.

Each phase is characterized by a series of mechanical parameters, thermally and geometrically specific to the phase being considered. These parameters are listed in Table 1.

Table 1
Global parameter of model

Percentage volume of phase
Size aggregate of each phase d_{max}
Young modulus, E and Poisson's ratio, ν
Tensile strength f_t
Compression strength f_c
Fracture energy G_f
Thermal dilation coefficient α_{th}
Coefficient of spherical and deviatoric coupling α_s
Damage hardening variable B_c
Thermal Conductivity λ
Specific heat C_p
Density ρ

3.2 The Macroscopic Damage Model MODEV

The considered thermo-mechanical coupled problem is governed by the following two equations (linear momentum and total energy conservation equations, respectively), in which the dot represents the derivative with respect to time,

$$\text{div}(\sigma) = 0 \quad (1)$$

$$\rho \dot{u} = \sigma : \dot{\varepsilon} - \text{div}(q) \quad (2)$$

and the small strains assumption has also been made. In these equations, σ represents the stress tensor, ε the strain tensor, u the density of internal energy rate, ρ the mass density and q the heat flux vector given by Fourier's law:

$$q = -\lambda \text{grad}(T) \quad (3)$$

where λ is the thermal conductivity, the aim of which is to account for thermo-mechanical degradation due to increase in cracking.

In order to model the isotropic phenomena of thermo elasticity and the damage within the framework of irreversible processes of thermodynamics, a specific set of state variables is used.

The Helmholtz free energy density, Ψ , is then considered as the thermodynamic potential, which is a function of all the state variables:

$$\Psi(\varepsilon, T, d, g) = \frac{1}{2} \varepsilon_{ij} : E_{ijkl}(d, g) : \varepsilon_{kl} - TC_{ij} : \varepsilon_{ij} - \frac{1}{2} C_p \frac{T_i^2}{T_0} \quad (4)$$

in which C_p is the specific heat and T_0 , the initial temperature of the system. The current material stiffness, fourth order tensor, E_{ijkl} , and the second order symmetric coupling tensor, C_{ij} , are given by

$$E_{ijkl} = \frac{\partial^2 \Psi}{\partial \varepsilon_{ij} \partial \varepsilon_{kl}} \quad \text{and} \quad C_{ij} = -\frac{\partial^2 \Psi}{\partial \varepsilon_{ij} \partial T} = 3K\alpha \cdot I \quad (5)$$

where E_0 is the initial stiffness tensor, K the bulk modulus, α the coefficient of thermal expansion and I the second order identity tensor. The independent state variables are therefore the total strain ε_{ij} , the relative temperature, $\cdot T_i = T - T_0$, the mechanical damage

variable d and the thermal damage variable g .

MODEV is a new deviatoric damage model. This model is based on the damage mechanics approach as well as the thermodynamics of Lemaître and Chaboche /10/, and it uses a non-symmetrical strain criterion.

Using the analogous model of Mazars /11/, and translating the local state of extension of the material, the model introduces two new equivalent strains local sliding and crack opening, respectively. They are calculated from the deviatoric and spherical parts of the strain tensors. The MODEV model considers two scalar damage variables that correspond to each degradation mechanism. Each damage variable has its own evolution law:

$$\varepsilon = \varepsilon^d + \varepsilon^s = \varepsilon^d + \varepsilon^H I \quad (6)$$

$$f(\varepsilon^s, K_s) = \tilde{\varepsilon}^s - K_s(D_s) = 0 \quad (7)$$

$$f(\varepsilon^d, K_d) = \tilde{\varepsilon}^d - K_d(D_d) = 0 \quad (8)$$

$K_h(D)$ and $K_d(D)$ are respectively the evolution functions of spherical and deviatoric damages. The equivalent spherical strain $\tilde{\varepsilon}^s$ and the deviatoric equivalent strain $\tilde{\varepsilon}^d$ are used to translate the local state of damage of the material and are defined as follows:

$$\tilde{\varepsilon}^d = \sqrt{(\varepsilon_1^d)^2 + (\varepsilon_2^d)^2 + (\varepsilon_3^d)^2} + \alpha \varepsilon^H \quad (9)$$

$$\tilde{\varepsilon}^s = \varepsilon^H \sqrt{3} \quad (10)$$

where ε_i^d are the Eigenvalues of the deviatoric strain tensor with $\alpha = 0.35$ being a coupling coefficient to take into account the hydrostatic effect. The initial yield function of damage for every type is identified by the available elementary tests, under uniaxial tension loading and pure shear loading.

$$\tilde{\varepsilon}_0^s = K_{0s}(D_s = 0) = \frac{f_t}{3 \cdot E} (1 - 2\nu) \quad (11)$$

$$\tilde{\varepsilon}_0^d = K_{0d}(D_d = 0) = \frac{\sqrt{2} f_{cis}}{2G} = \frac{\sqrt{2} f_t}{E} (1 + \nu) \quad (12)$$

where E , G , ν , f_t , f_{cis} are respectively the Young modulus, the shear modulus, the Poisson's ratio, strength tensile and shear strength.

In order to have a continuous solution with respect to thermodynamics, the yield surface is convex and contains the origin. The criteria are drawn from the principal strain space, shown in Fig. 3. The global macroscopic mechanical damage, computed at every point material, is deduced by combining the 2 damage variables:

$$(1-d_{\text{macro}}) = (1-D_s)(1-D_d) \quad (13)$$

The law of evolution of the damage variable defines the variation of the yield surface of damage, which is a function of the equivalent strain. We modify the evolution laws according to Mazars /11/ by adapting them to the characteristics of MODEV'S mode:

$$d_s = 1 - \frac{\tilde{\varepsilon}_0^s}{\tilde{\varepsilon}^s} \exp\left[-B_t (\tilde{\varepsilon}^s - \tilde{\varepsilon}_0^s)\right] \quad (14)$$

$$d_d = 1 - \exp\left[-B_c (\tilde{\varepsilon}^d - \tilde{\varepsilon}_0^d)\right] \quad (15)$$

Where B_c and B_t are the two hardening parameters of the model respectively in compression and traction. The B_t parameter is linked to the fracture energy G_f by:

$$B_t = l_c \frac{f_t}{G_f} \quad (16)$$

where l_c is the characteristic length and f_t is the tensile strength.

To obtain the objective results with regard to the mesh, Hillerborgs' method /12/ was adopted. This method consists of introducing the fracture energy into the FE model by calculating the softening branch of the tension law.

Due to the nature of the total secant initial formulation, the MODEV model was not able to take into account the inelastic permanent strain observed when testing under tension and compression loading. The inelastic permanent strain in tension is mainly due to the imperfect crack closing. This phenomenon is caused by the roughness of the crack lips, which prohibits a perfect contact after the first opening. The heterogeneity of the concrete and the presence of aggregates can explain this. Consequently, in compression, the MODEV model postulates that the damage mechanism is induced by deviatoric strain and causes a sliding dislocation.

It now becomes necessary to assess the tangent operator of the stiffness matrix. This tangent operator allows us to define the relationship between the strain and stress increments. The stress-strain relationship in its total formulation can be written as follows:

$$\sigma_{ij} = (1-d_s)(1-d_d) E_{ijkl} \varepsilon_{ij} \quad (17)$$

4. STUDY OF THERMAL DAMAGE

4.1 Thermal Damage Due to Restrained Thermal Strain

As described above, the thermal damage due to restrained thermal strain is broken down into macroscopic damage d_{macro} and microscopic damage d_{micro} . The global thermal damage is obtained by the following combination:

$$d = 1 - (1-d_{\text{micro}})(1-d_{\text{macro}}) \quad (18)$$

Figure 4 shows the DC simulated evolution of damage in a free concrete sample - whose size is 10 times larger than that of the coarser aggregate at 423 K.

4.2 Thermal Damage due to Physical/Chemical Transformations

This damage was represented in the model by introducing the so-called g damage variable. The evolution of this variable is obtained directly from the previously conducted tests on cement paste samples. To define this function, the effects of the elastic modulus are used because they are the most appropriate with respect to the relationship between high temperatures and mechanical properties. Assuming that the relationship between the reduced and the original elastic modulus is proportional to the thermal damage variable, experimental curves relating the elastic modulus to the temperature can be used to express this function as:

$$g(T) = 1 - \frac{E(T)}{E_0} \quad (19)$$

The damage variable, g , has been identified experimentally from a test performed on free cement samples. Note that $E(T)$ is obtained by three-point

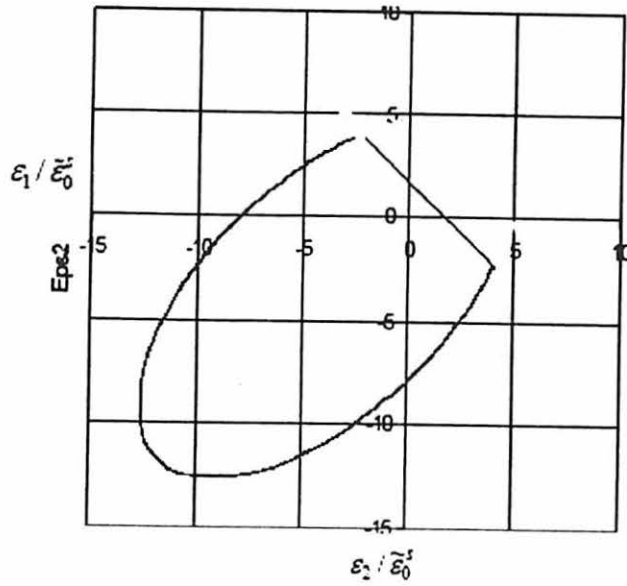


Fig. 3: MODEV damage yield surface

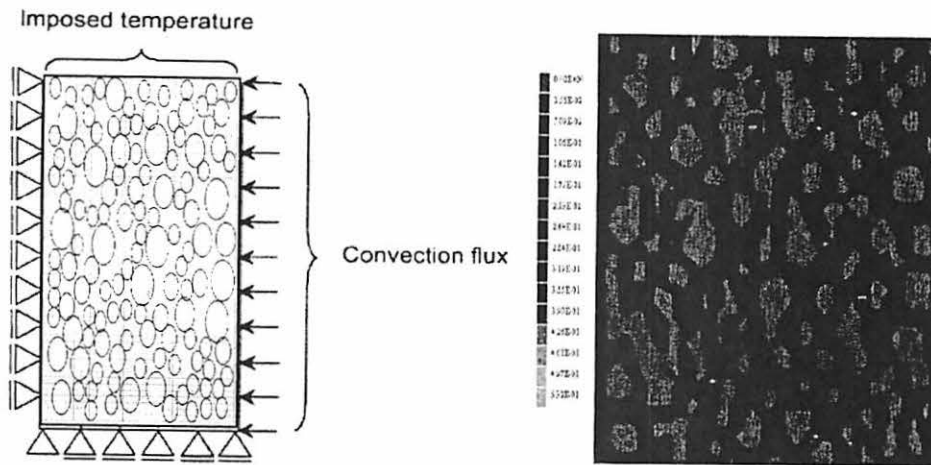


Fig. 4: Finite element mesh micromechanical damage exemple with DC model at 423 K

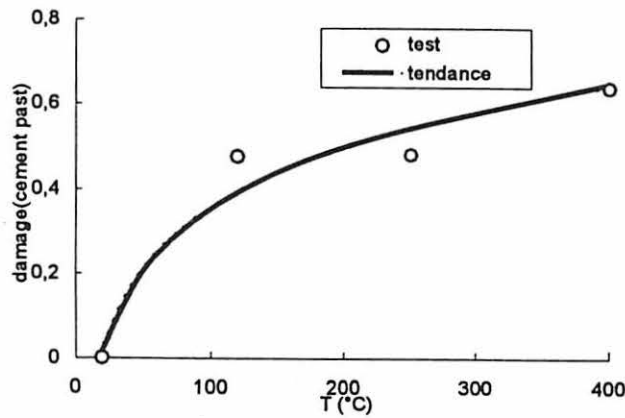


Fig. 5: Physical and chemical thermal damage origin

bending tests on specimens that have been heated at different temperatures and then cooled progressively in order to avoid additional degradation due to quick cooling.

Figure 5 shows the g function, which was obtained by fitting the experimental results that were introduced into DC model. This function can be written as follows:

$$g(T) = 0.2 \cdot \ln(T) - 0.6, \quad g(T) \in [0, 1[\quad (20)$$

Finally, it is concluded from this that the total damage, as described in Fig. 6, can be written as follows:

$$1 - D = (1 - d)(1 - g) \\ = \underbrace{(1 - D_S)}_{\text{macro}} \underbrace{(1 - D_d)}_{\text{dilatation}} \underbrace{(1 - d_{\text{micro}})}_{\text{chemical}} \underbrace{(1 - g)}_{1-g} \quad (21)$$

5. MODEL VALIDATION

The validation of the model was done by comparing the experimental test results on cement mortar and concrete samples. The goal of this experimental study was threefold: to provide the physical and chemical damage function g , to validate the numerical multi-scale homogenization, and to evaluate the accuracy of this approach.

To do this, five materials were tested: cement paste, high-strength mortar (HSM), ordinary concrete (OC), and two types of high-strength concrete (HSC). All materials were tested using notched beam samples, previously heated according to the RILEM recommendations /13/, and subjected to three-point bending moments in order to produce fully stable test results. For each material, 3 notched beam samples, with dimensions $100 \times 100 \times 400 \text{ mm}^3$, were tested until failure. All samples were tested at 293 K after having undergone a heating cycle with the following temperatures: 293 K, 393 K, 523 K or 673 K. A temperature rate of 0.5 K/min was adopted for the heating and cooling phases. The speed of heating and cooling was optimized by simulation in order to avoid any mechanical damage through the effect of the temperature gradient and to allow for the moisture transport processes to develop.

It is assumed that the chemical reactions and transformations will mainly take place in the cement paste (for temperatures ranging from 293 K to 673 K). Thus, from the experimental results obtained on the cement paste (g function), the damage behavior can be reproduced by simulation for the mortar and also for the various concrete materials.

After these simulations, a comparison between the numerically predicted laws and those obtained by experiments is studied. The comparison that is presented in this article applies to 3 of the 5 materials tested in the work of Menou /14/.

5.1 Mortar Results

The test concerns a notched mortar beam sample, with cut dimensions ($100 \times 100 \times 400 \text{ mm}^3$). The sample is slowly heated at a rate of 0.5 K/min until 673 K is reached. For modelling this test with the DC model, the mortar was considered as a two-phase material: one phase of cement paste and n phases of sand aggregates defined according to the graduation of the material.

Figure 7 shows the generation of the heterogeneous material with the DC model. The modelling of the temperature evolution is done by considering a transient thermal simulation with the applied boundary conditions on the body of the test sample (0,5 K/min).

Fig. 8 shows the iso-levels of the thermal damage at 673 K. Fig. 9 shows a comparison between experimental results and simulation.

The results of the simulation were also compared with test results of three bending points undertaken by Sullivan and al. /15/. on mortar samples tested for residual and hot modulus as shown in Fig. 10. The simulation shows that the damage is almost steady between 393 and 523 K. This was also observed experimentally by Sullivan et al /15/. It is necessary to note that at this level of temperature, the difference between the thermal expansion coefficient of cement paste and aggregates is very small. This explains the non-evolutionary behavior of damage at this level and also confirms the local mechanical origin of the thermal damage. The thermal damage function obtained by simulation (Fig. 5) will be introduced thereafter into the model in order to homogenize the concrete.

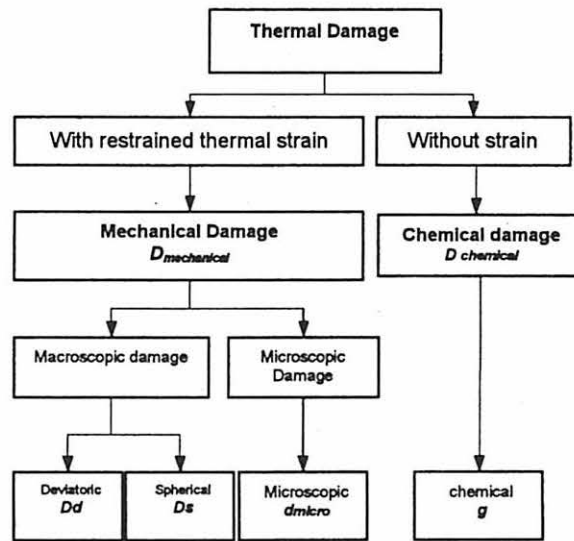


Fig. 6: Thermal damage approach of concrete

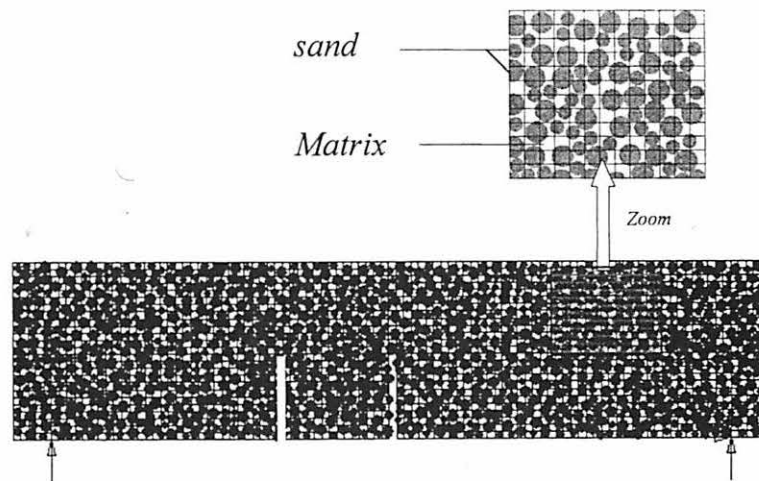


Fig. 7: Generation and boundary conditions (mortar)

5.2 Results on Ordinary Concrete and High-Strength Concrete

As for mortar, the concrete test samples measuring $100 \times 100 \times 400 \text{ mm}^3$ were heated slowly at a rate of 0.5 K/min until reaching 673 K . The tests were modelled with plain stress hypotheses while considering, in this case, the concrete is a two-phase material: the homogenized mortar (made of cement paste and sand aggregates) and n phases of different size grading according to the composition of the material

The mechanical loadings were applied by prescribing displacements after thermal loading. Figure 11 shows the generation of the heterogeneous material with the DC model, as well as the mechanical boundary conditions.

The results of simulation that are presented here concern two different concretes:

- Ordinary Concrete (OC)
- High-Strength Concrete (HSC)
-

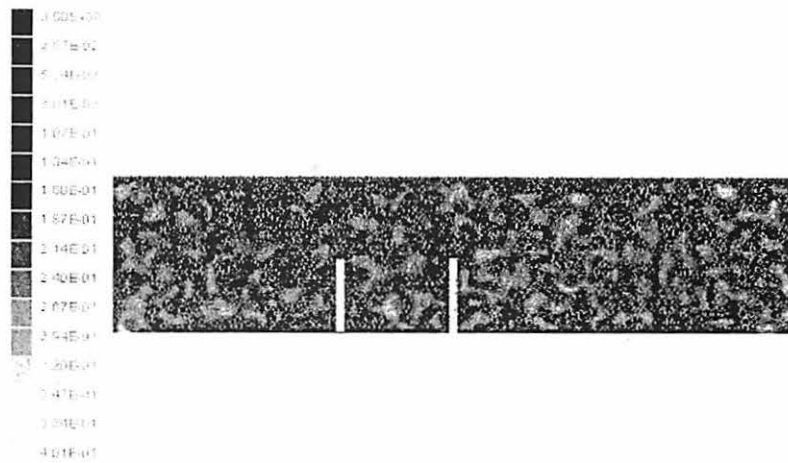


Fig. 8: Mortar thermal damage state with DC (Digital Concrete)

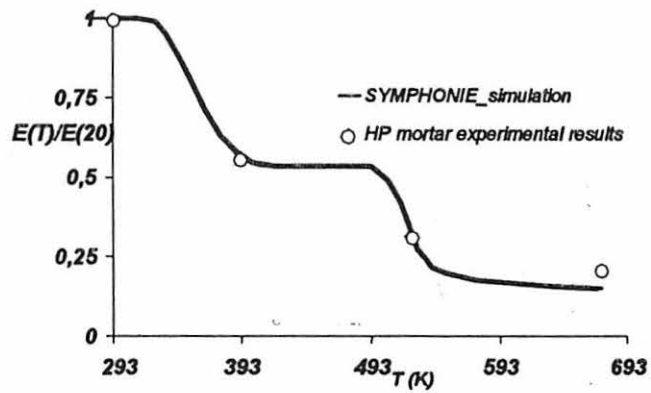


Fig. 9: Comparison between HSM experimental thermal damage and results of simulation

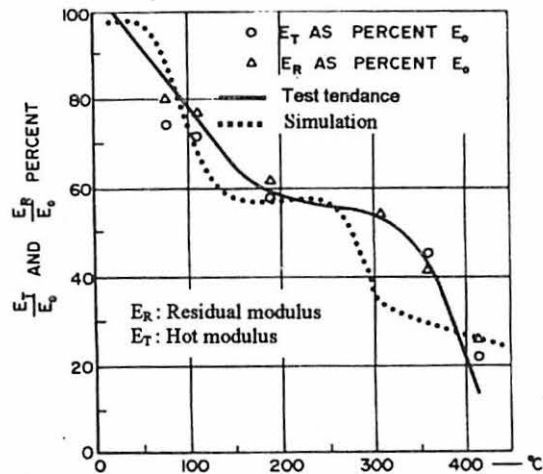


Fig. 10: Evolution of the modulus ordinary concrete at high temperature (flexure test /16/)

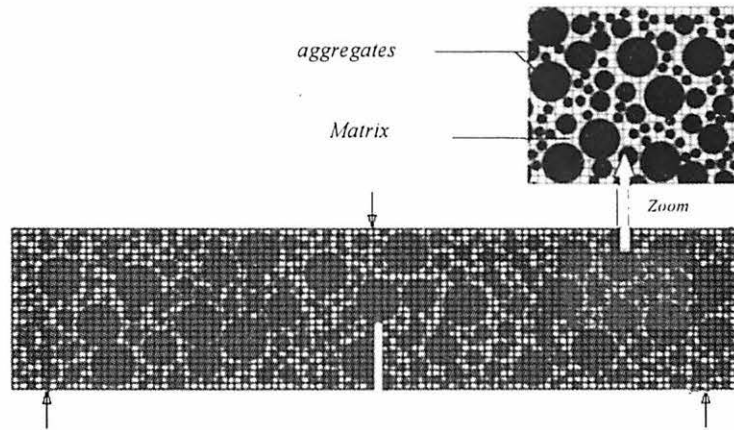


Fig. 11: Generation and boundary conditions (Concrete)

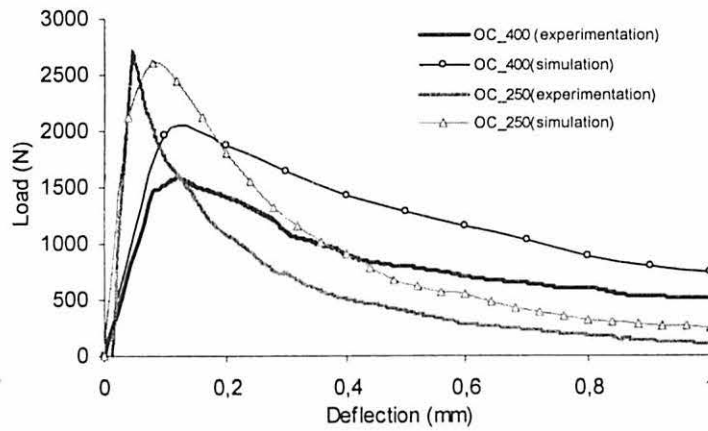


Fig. 12: Load-deflection at 523 and 673 K (OC)

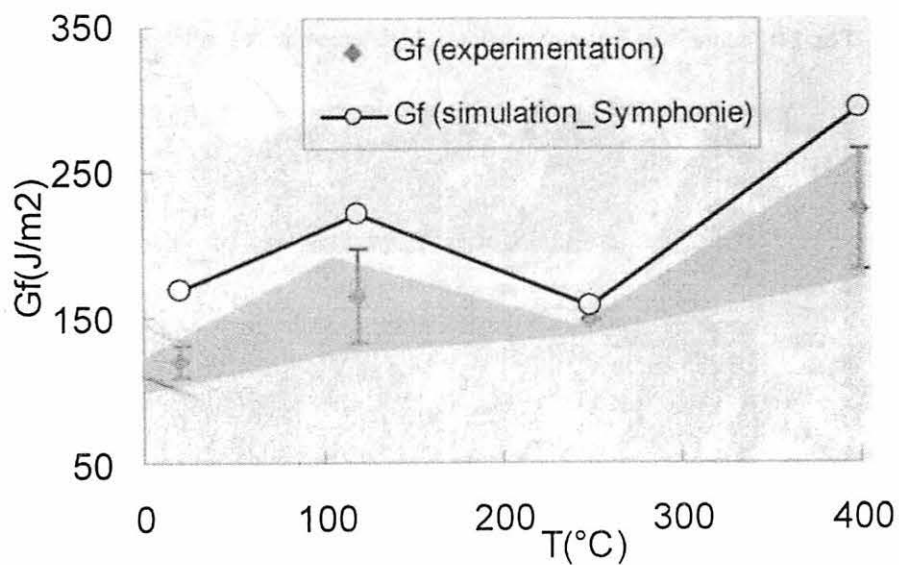


Fig. 13: Experimental evolution of the fracture energy $G_f/8/$ compared to the predicted evolution by simulation.

a. Ordinary Concrete results

Fig. 12 shows the experimental and simulated load-displacement curves of the OC at both 523 K and 673 K.

Fig. 13 shows the ultimate loads at failure, obtained respectively by simulation and by testing according to the temperature. The comparison with the experimental results shows promising accuracy.

Fig. 14 shows the evolution of the fracture energy of the OC generated by simulation and compares it to the experimental tests at different temperature levels. It is noted that values of G_f obtained by simulation are very

close to those given by tests.

Fig. 15 shows the iso-levels of damage obtained simulation on SYMPHONIE at 393 K and 673 K.

b. High-Strength Concrete Results

Fig. 16 shows the experimental and simulated load displacement curves of the HSC at 523 K and 673 K.

Fig. 17 shows the experimental and predicted ultimate loads at failure for the different values of temperature.

Fig. 18 shows a comparison between the experimental fracture energy and the simulated fracture

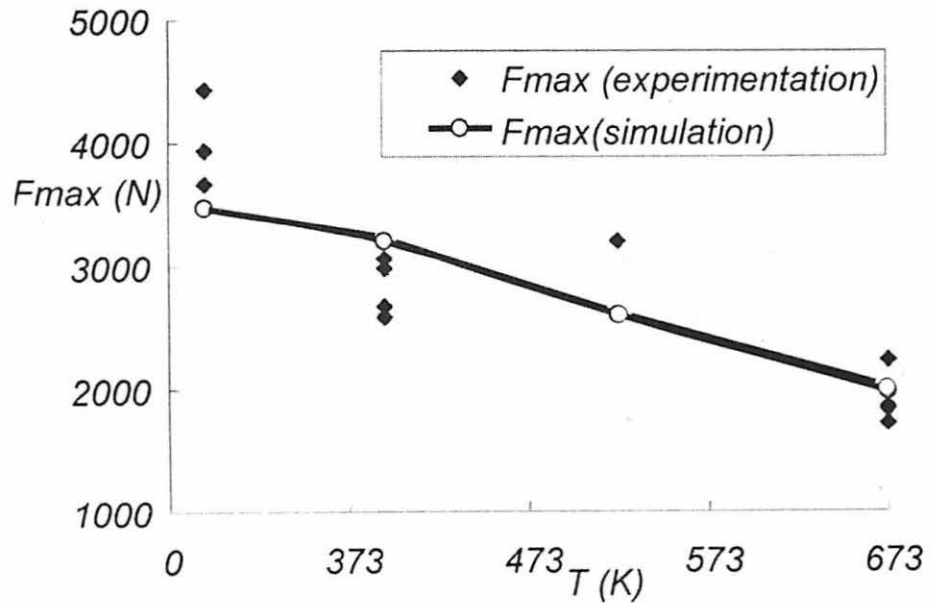


Fig. 14: Failure load Fmax simulation at high temperature (ordinary concrete)

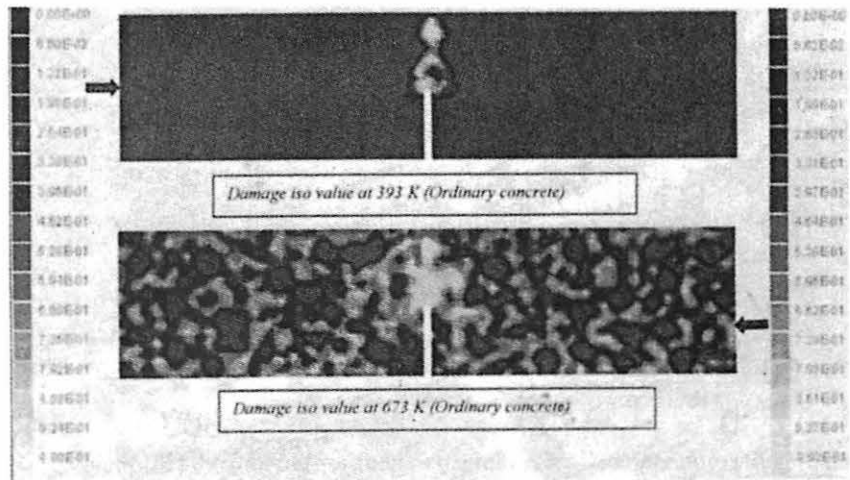


Fig. 15: Thermal damage iso-value at 373 and 673 K (ordinary concrete)

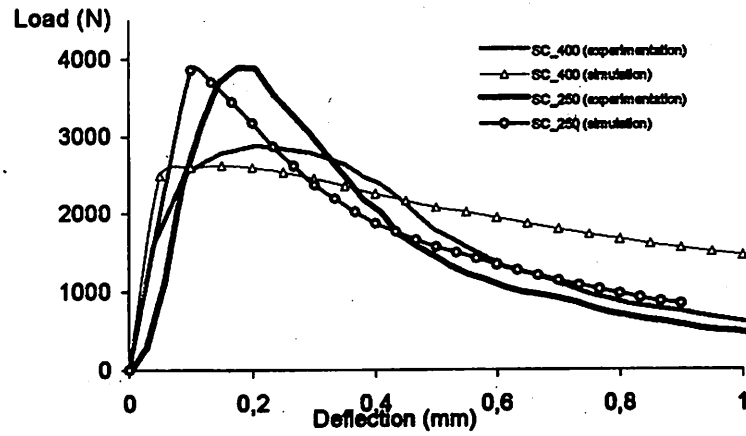


Fig. 16: Load-deflection at 523 and 673 K (HSC)

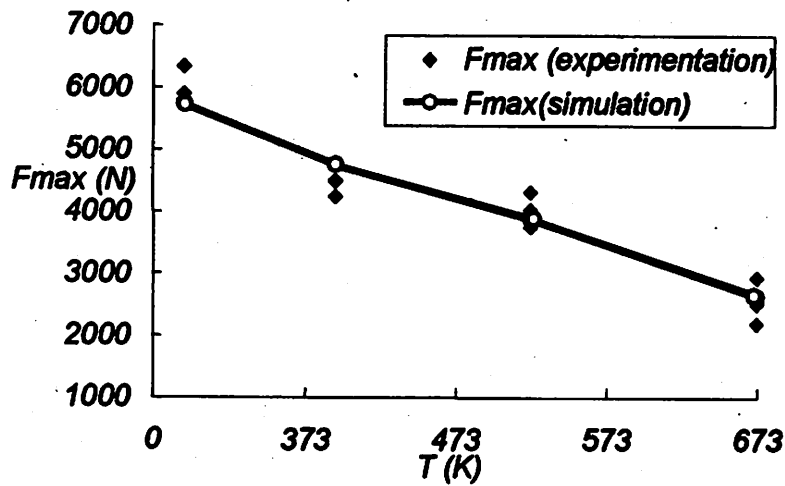


Fig. 17: Experimental and predicted values of ultimate loads at different temperature levels for HSC.

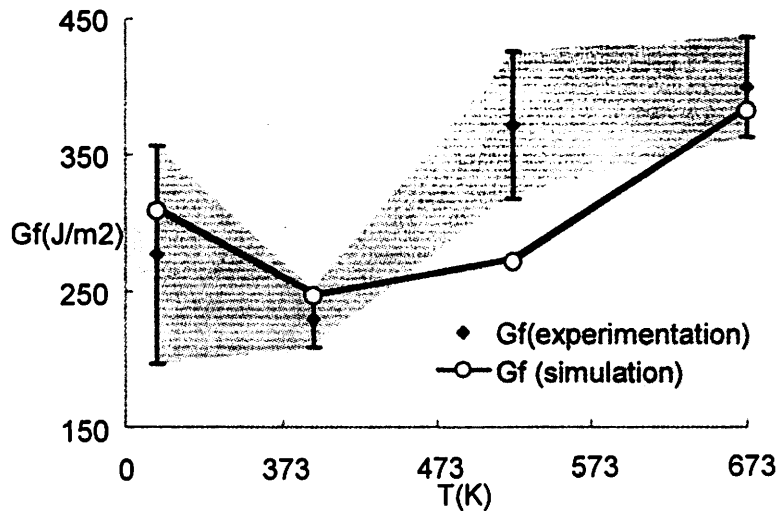


Fig. 18: Predicted Fracture energy G_f by simulation and comparison with experimental results

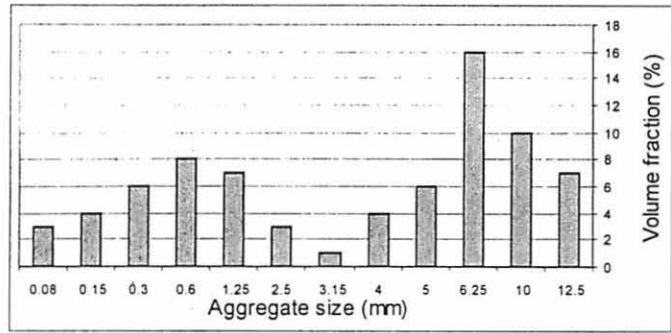


Fig. 19: Aggregate size distribution adopted for the simulations.

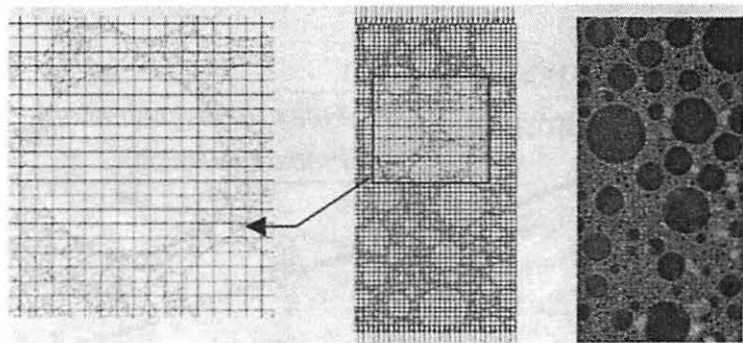


Fig. 20: Mesh and boundaries conditions; Thermal damage after one hour

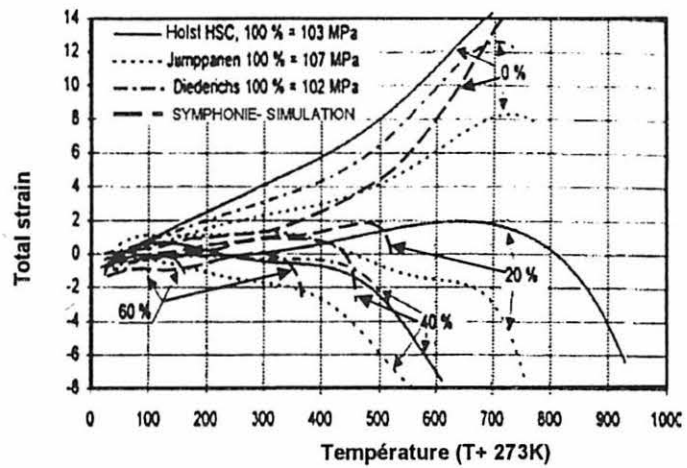


Fig. 21: Model response for coupled thermal and mechanical loads compared to tests results (up to 773 K)

energy as a function of temperature for the HSC.

The tests demonstrated that the cementitious materials behaved almost identically when the fracture energy G_f is considered as a function of maximum temperature. The thermal damage due to heating from 393 to 673 K. increases the fracture energy by 50% according to the reference tests at room temperature. A more tortuous crack surface is one reasonable explanation for the significant increase in G_f . It is demonstrated by simulation, that the temperature exposure makes all cementitious materials tested, significantly more ductile and less resistant.

6. SIMULATION OF CONCRETE SPECIMENS SUBJECTED TO COMPRESSIVE LOADS AT HIGH TEMPERATURE

To study the thermal damage of concrete specimens when they are heated under compressive load, the experimental tests carried out by Holst /16/ were simulated. Cylindrical specimens (136 x132mm²), were subjected to several constant compressive loads and heated to 1073 K at a heating rate of 4.98 K/min.

The tests were modelled in 2D, using an axisymmetrical model. A constant compressive load was applied at the top of the specimen at the beginning of the heating stage and was maintained during the test. The loads represent 0%, 20%, 40% and 60% of the compressive strength of the HSC (108 MPa). **Figure 19** shows the geometry, the mesh and the boundary conditions adopted for the computations. The thermo-mechanical characteristics of the HSC were given by Holst /16/. To perform the computations with the Digital Concrete model, it is also necessary to know the properties of cement paste and aggregates separately (tensile and compressive strengths, thermal expansion coefficient, fracture energy, Young modulus...) with most of these being chosen from literature (see Bazant and Kaplan /17/ and Diederichs *et al.* /2/). The material parameters and their values, used in the simulation, are presented in Table 2, where E is the Young modulus, f_t the tensile strength, f_c the compressive strength, α_{th} the thermal dilation coefficient, β_c the damage hardening variable, G_f the fracture energy and ν the Poisson's ratio. The aggregate size distribution of the concrete is described in **Fig. 20**.

Table 2
Materials parameters defined for the cement paste and for concrete aggregates.

	E (Mpa)	ν	f_t (Mpa)	f_c (Mpa)	G_f (N/mm)	α_{th} (K ⁻¹)	B_c
Cement Paste	20000	0.2	4	15	0.1	0.3	80
Aggregates	80000	0.28	10	20	0.15	0.3	70

The evolution of the thermal expansion coefficients (α_{th}) of concrete components (cement paste and aggregates) with temperature is given in Tables 3 and 4. The thermal damage in the specimen, obtained after one hour of heating, is presented in **Fig. 19**. The damage computed, using a macroscopic model, was often very small compared to the damage obtained at the constituent's scale, using the DC micromechanical approach. This damage is mainly due to the strong difference between the coefficients of thermal expansion of the cement paste and the aggregates; a uniform temperature variation generates strain gradients

in the material which is now analyzed as a structure. These strain gradients are responsible for the resulting damage zones at the small level. Simulations and experimental results are in good agreement. **Figure 21** presents for the simulations and experiments, the evolution of the total strain versus the temperature for the 4 loading levels (0, 20, 40 and 60%). These results confirm that the evolution of the total strain is mainly due to the thermal degradation of the concrete stiffness at high temperature. No additional strain component, such as transient or creep strain, is needed to explain the evolution of the total strain versus temperature.

Table 3
Thermal expansion coefficient of cement paste

T (K)	α_{th} (K ⁻¹)
293	10 e-6
393	15 e-6
673	-5 e-6
1473	-25 e-6

Table 4
Thermal expansion coef. of aggregates

T (K)	α_{th} (K ⁻¹)
293	3 e-6
473	9 e-6
773	21 e-6
1073	57 e-6

In order to understand the mechanisms leading to the deterioration of concrete under the effect of combined compressive and thermal loading, and to show the structural effect of such loading, numerical micro-mechanical simulations of the experimental tests carried out by Holst /16/ were achieved at the micro scale. These simulations show that the experimental "transient strain of concrete" do not reflect an intrinsic material behaviour, but should be considered as structural behaviour due to both the restrained boundary conditions and the microscopic thermal damage.

7. CONCLUSION

A multi-scale simulation using a DC model was conducted on 4 cement-based materials: a High-Strength Mortar (HSM), an Ordinary Concrete (OC), and two types of High-Strength Concrete (HSC).

A comparison between experimental results and the simulation was presented. This comparison shows a good agreement between experiments and simulation for all of the materials tested. These results confirm the relevance of the multi-scale approach to predict the total behaviour of cement-based materials and to quantify their thermal damage. This approach allows a better understanding of the original elementary mechanisms of the thermal damage evolution of concrete at high

temperatures, and to clearly separate the mechanical damage (at micro and macro levels) from the physical and chemical damage. We can consider that the micro-mechanical damage of concrete mainly concerns the difference between the characteristics of the aggregates and the cement paste while the physical/chemical thermal damage mainly occurs in the cement paste.

The final set of simulation results in this article confirm that, the evolution of the total strain of concrete specimens when subjected to such loading is mainly due the thermo mechanical degradation of the concrete's properties at high temperatures. Therefore, no additional strain component, such as transient or creep strain, is needed to obtain the evolution of the total strain versus temperature.

The next research step in the present work is now focused on the study of the effect that the size grading has on the fracture energy and on the estimation of the porosity and the permeability of concrete related to the cement-water ratio.

REFERENCES

1. Z.P. Bazant and C. Part, *ACI Materials Journal*, Technical paper Title No. 85-M32 (1988).
2. U. Diederichs, U-M Jumpanen. and V. Penttala, *Helsinki University of Technology, Department of Structural Engineering*, Report 92. p.723, 1992.
3. F.J. Ulm, O. Coussy and Z.P. Bazant, *Journal of Engineering Mechanics*, March, 272-282 (1999).
4. A.M. Brandt, *Cement-based Composites: Materials, Mechanical Properties and Performance*. UK: E & FN Spon, 1995.
5. JGM.Van Mier *Fracture Processes of Concrete: Assessment of Material Parameters for Fracture models*. USA: CRC Press, 1997.
6. M.G.A. Tjissens, L.J. Sluys and E.V.D. Giessen *Engineering Fracture Mechanics Journal*; 68:1245-63 (2001).
7. G. Mounajed, SYMPHONIE, *Software F.E, CSTB*, France. <http://mocad.cstb.fr>, (1991).
8. G. Mounajed, A. Menou, H. Boussa, Ch. La Bordrerie and H. Carré *Proceedings of the Fifth International Conference on Fracture Mechanics of Concrete and Concrete Structures*, Vol. 1, pp 513-520, Vail Colorado, USA, 2004.

9. A. Menou, G. Mounajed, H. Boussa, A. Pineaud and H. Carre. *Theoretical and Applied Fracture Mechanics*, Volume 45, 1, pages 64-71, 2006.
10. J. Lemaître and J.L. Chaboche, *Mécanique des matériaux solides*. Dunod Edition, France, 1988.
11. J. Mazars, *PhD Thesis, University of Paris VI*, (1984).
12. A. Hillerborg, M. Modéer and P.-E. Petersson, *Cement and Concrete Research*, B6B(6), 773-781 (1976).
13. RILEM Committee FMC 50, *Material and Structures*, Vol 18, N° 106 (1985).
14. A. Menou, *PhD Thesis Pau et Pays de l'Adour University*, France, 2004.
15. P. J. E. Sullivan and M. P. Poucher, *ACI Publication SP 25*, PP 103- 135. (1971).
16. F. Holst.. High Performance Concrete, *Interim Report, M7 :2*, Division of Building Materials, ²LTH, Lund, Finland (1994).
17. Z.P. Bažan and M.F. Kaplan, *Concrete at High Temperatures: Material Properties and Mathematical Models*, Longman Group Limited., London, 1996.